Title
Designing accelerator-based epithermal neutron beams for BNCT

Author
Bleuel, D.L.

Publication Date
1997-07-01

LBNL-40551 Rev.
UC-406

ERNEST ORLANDO LAWRENCE
BERKELEY NATIONAL LABORATORY

Designing Accelerator-Based Epithermal Neutron Beams for BNCT

D.L. Bleuel, R.J. Donahue,
B.A. Ludewigt, and J. Vujic

Accelerator and Fusion Research Division

July 1997

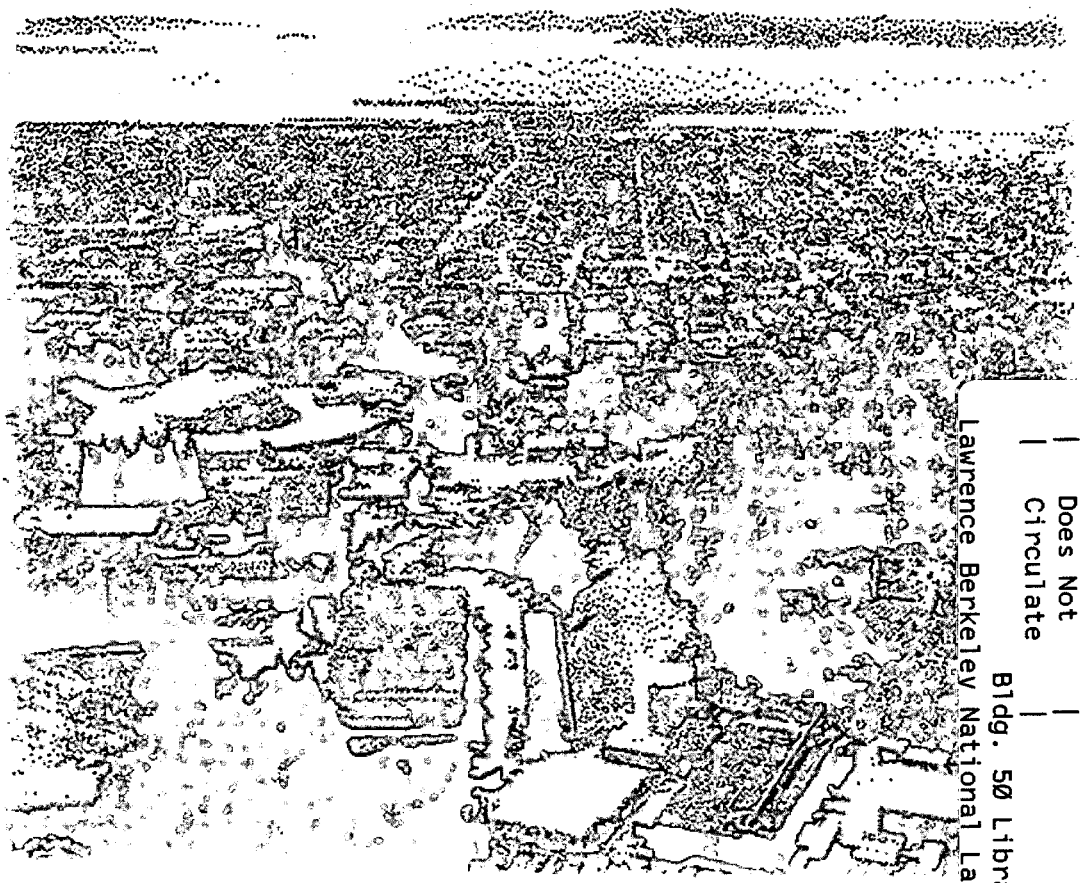

DISCLAIMER

LBNL-40551 Rev.
UC-406

Designing Accelerator-Based Epithermal Neutron Beams for BNCT

D.L. Bleuel,[a,b] R.J. Donahue,[a] B.A. Ludewigt,[a] and J. Vujic[b]

[a]Accelerator and Fusion Research Division
Ernest Orlando Lawrence Berkeley National Laboratory
University of California
Berkeley, California 94720

[b]Department of Nuclear Engineering
University of California, Berkeley, California 94720

July 1997

This work was supported by the Office of Health and Environmental Research, Office of Energy Research, of the U.S. Department of Energy under Contract No. DE-AC03-76SF00098.

LBNL-40551 Rev
UC-406

Designing Accelerator-Based Epithermal Neutron Beams for BNCT

D. L. Bleuel[a,b], R. J. Donahue[a], B. A. Ludewigt[a], J. Vujic[b]

[a]E. O. Lawrence Berkeley National Laboratory, Berkeley, CA 94720
[b]Nuclear Engineering Department, University of California, Berkeley, CA 94720

Abstract

The $^{7}Li(p,n)^{7}Be$ reaction has been investigated as an accelerator-driven neutron source for proton energies between 2.1 MeV and 2.6 MeV. Epithermal neutron beams shaped by three moderator materials, Al/AlF_3, ^{7}LiF, and D_2O, have been analyzed and their usefulness for Boron Neutron Capture Therapy (BNCT) treatments evaluated. Radiation transport through the moderator assembly has been simulated with the Monte Carlo N-Particle code (MCNP). Fluence and dose distributions in a head phantom were calculated using BNCT treatment planning software. Depth-dose distributions and treatment times were studied as a function of proton beam energy and moderator thickness. It was found that an accelerator-based neutron source with Al/AlF_3 or ^{7}LiF as moderator material can produce depth-dose distributions superior to those calculated for a previously published neutron beam design for the Brookhaven Medical Research Reactor achieving up to ~50% higher doses near the mid-line of the brain. For a single beam treatment, a proton beam current of 20 mA, and a ^{7}LiF moderator the treatment time was estimated to be about 40 minutes. The tumor dose deposited at a depth of 8 cm was calculated to be about 21 Gy-Eq.

Key words: BNCT, accelerator, epithermal neutron beam, moderator design

---

This work was supported by the Office of Health and Environmental Research, Office of Energy Research of the U.S. Department of Energy under Contract Number DE-AC03-76SF00098.

I. INTRODUCTION

Research in Neutron Capture Therapy (NCT) is motivated by the desire to find an alternative therapy for malignancies where conventional radiation therapies fail, such as glioblastoma multiforme (GBM), a malignant brain tumor. Boron Neutron Capture Therapy (BNCT), the most advanced form of NCT, relies on a binary method for delivering a sufficient dose to the tumor cells without exceeding the healthy brain tolerance. A pharmaceutical compound which carries ^{10}B and concentrates selectively in the malignant tissues is administered to the patient, who is subsequently irradiated with an external neutron beam. ^{10}B has a very large capture cross section of 3830 barns for thermal neutrons and decays into an alpha particle and a lithium ion with an accompanying 480 keV γ ray in 93% of the reactions. The combined range of the decay products is less than 10 μm, thus confining their dose contributions largely to the cells which contain ^{10}B. The success of this therapy depends on two factors, the efficiency of a drug to deliver ^{10}B preferentially to the malignant cells and the availability of an epithermal neutron beam to provide a sufficient thermal neutron flux at the depth of the tumor.

At present, clinical BNCT trials for high-grade primary brain tumors (GBM) are ongoing at the Brookhaven Medical Research Reactor (BMRR)[1] and at the Massachusetts Institute of Technology Research Reactor. As an alternative to nuclear reactors, accelerator-based neutron sources are being studied for future use at hospitals. Such sources offer the potential for improved patient treatments in addition to avoiding problems associated with new reactor installations. The maximum neutron energy from an accelerator-based neutron source utilizing the $^{7}Li(p,n)^{7}Be$ reaction is significantly below fission neutron energies thus requiring less moderation. As discussed below in Sec. VI and VII this can be exploited to achieve clinically superior depth dose distributions. Furthermore, proton beam energy, moderator, and neutron beam collimation can rather easily be changed to optimize the neutron beam for a particular treatment.

An accelerator-based BNCT facility is under development at the Lawrence Berkeley National Laboratory (LBNL)[2]. The $^{7}Li(p,n)^{7}Be$ reaction at proton energies of about 2.5 MeV will be utilized since it offers a high neutron yield in combination with a low maximum neutron energy. The d.c. accelerator design features an electrostatic quadrupole (ESQ) column which is ideally suited for high beam current and high reliability operation[3]. The electrostatic quadrupole lenses provide the key advantage of

strong transverse focusing without a longitudinal field near the breakdown limit. The acceleration column[4] has been designed for a proton beam current of 100 mA. A new power supply, an air-core multistage transformer-rectifier stack[5], will allow operation at currents exceeding 50 mA. The size of such an accelerator, less than 5 m in length and 2 m in diameter including the power-supply, is suitable for housing in a hospital. Other accelerators with lower maximum beam currents have been proposed for BNCT or are under development[6,7].

A crucial component of the accelerator-based neutron source is the neutron production target. Because metallic lithium has a low melting point of 179°C, very effective target cooling is mandatory. A target has been designed featuring a lithium layer deposited on an aluminum backing. This layer is of sufficient thickness to lower the proton energy to below the reaction threshold taking the incident beam angle into account, e.g., 50 μm for a 30° angle. Following the microchannel absorber concept[8], many channels are cut into the aluminum substrate for convective water cooling. The results of a finite element analysis and a recent heatload test of a prototype aluminum panel at the Plasma Materials Test Facility at Sandia National Laboratory indicate that for a heatload of ~600 W/cm^2 the surface temperature can be kept below 150°C. Further analyses showed that beam currents exceeding 50 mA can be handled by using a target area up to 15 cm x 15 cm and placing the target panels at a 30° angle in respect to the beam. The target will be followed by a moderator assembly which shapes the neutron energy spectrum and optimizes the epithermal neutron beam for the clinical application.

The aims of the study presented in this paper were twofold: first, to determine accelerator and target specifications starting from clinical requirements and second, to study the design of epithermal neutron beams for the treatment of deep-seated intracranial tumors. Sec. II describes the modeling of the ^{7}Li(p,n)^{7}Be reaction and calculation of energy and angular distribution of neutrons emitted from production target as a function of incident proton kinetic energy. Epithermal neutron beam shaping by three moderator materials (Al/AlF_3, ^{7}LiF, D_2O) is analyzed in Sec. III. Sec. IV presents the clinical requirements adopted for our study and discusses figures-of-merit for the optimization of epithermal neutron beams. Depth-dose distributions and treatment times as a function of proton beam energy, type of moderator, and moderator thickness are presented in Sec. V. Also discussed are the assumptions and uncertainties in the Monte Carlo modeling of the neutron and γ transport. The analysis of the results and conclusions are given in Sec. V and VI, respectively.

II. MODELING OF THE $^7Li(p,n)^7Be$ REACTION

The reaction $^7Li(p,n)^7Be$ displays a large resonance in the forward direction around 2.3 MeV which extends to about 2.5 MeV. It has been generally accepted that the highest neutron yields for BNCT are obtained at a proton beam energy of 2.5 MeV. However, there is a tradeoff between total neutron yield and maximum neutron energy. The $^7Li(p,n)^7Be$ cross sections[9] exhibit a large high-energy tail increasing with the incident proton energy.

Double differential (angle and energy) neutron yield distributions were calculated as a function of incident proton beam energy using center-of-mass best values for normalized Legendre coefficients[9] for predicting cross sections for the $^7Li(p,n)^7Be$ reaction. For a given proton energy the cross section, as a function of center-of-mass angle ϕ, can be determined in the center-of-mass system by:

$$\frac{d\sigma}{d\omega}(\phi) = \frac{d\sigma}{d\omega}(0°)\sum_i A_i P_i(\phi) \qquad (1)$$

where A_i are the coefficients of the Legendre polynomials determined by Liskien and $P_i(\phi)$ are the Legendre polynomials.

After transformation into the laboratory system the neutron energy is determined by the following relation[10]

$$E_n = E_p \frac{m_p m_n}{(m_n+m_p)^2} \{ 2\cos^2\theta + \frac{m_r(m_r+m_n)}{m_p m_n} [\frac{Q}{E} + \frac{1-m_p}{m_r}]$$

$$\pm 2\cos\theta \sqrt{\cos^2\theta + \frac{m_r(m_r+m_n)}{m_p m_n} [\frac{Q}{E} + \frac{1-m_p}{m_r}]} \} \qquad (2)$$

where E_n and E_p are the neutron and proton kinetic energies, m_n and m_p their respective masses, m_r the residual target mass (i.e., ^7Be), and θ the scattering angle. The Q-value for this reaction is 1.644 MeV[9]. The reaction thresholds are given by Liskien as 1.881 MeV in the forward direction and 1.920 MeV in the backward direction. The threshold, which is used to determine the target thickness, is assumed to be 1.950 MeV as this is as low as Liskien's Legendre coefficients were fitted to experimental data.

Only the reaction $^{7}Li(p,n)^{7}Be$ is considered. The reaction $^{7}Li(p,n)^{7}Be^{*}$ which produces a 0.431 MeV γ ray with a threshold of 2.373 MeV in the forward direction and 2.423 MeV in the backward direction is not considered in our treatment. This cross section is generally only a few percent of the $^{7}Li(p,n)^{7}Be$ cross section at proton energies less than or equal to 2.5 MeV. The target thickness is calculated by subtracting the range of the incident proton from the range of a proton at the threshold energy in lithium metal. In this way only protons with energies at or above the reaction threshold are allowed to deposit any energy directly in the target to minimize heating of the target. Range and stopping power data are taken from Janni[11] with log-log interpolation for intermediate energy values.

The target is then subdivided into many equal-thickness regions. In each region the proton beam energy is determined, the Legendre coefficients are sampled and the cross sections are determined over 1° angular increments. For each subregion a check is made to ensure that

$$\sigma = \int_0^{2\pi}\int_0^{\pi} \frac{d\sigma}{d\omega_L} = \int_0^{2\pi}\int_0^{\pi} \frac{d\sigma}{d\omega_C} = 4\pi \frac{d\omega}{d\omega}(0°)\ A_0 \qquad (3)$$

where $d\omega_L$ and $d\omega_C$ are the lab system and center-of-mass system differential solid angles.

For each proton energy and each sampled angle the neutron energy is calculated from Eq. (2). From this the overall double differential neutron production probabilities can be estimated for each incident proton beam energy. As an example the neutron energy spectra for various incident proton energies are shown in Fig. 1. This figure shows only those neutrons produced in the forward 30° cone with respect to the proton beam. The total neutron yields per incident proton are $5.45\ 10^{-5}$, $9.26\ 10^{-5}$, and $1.23\ 10^{-4}$ for proton energies of 2.2, 2.3, and 2.4 MeV, respectively. More details and calculated neutron spectra for different angle bins can be found in Ref. 12. The output from this program, for all neutron energies and angles, is used as the starting point for subsequent simulations of neutron transport in various moderator and reflector materials.

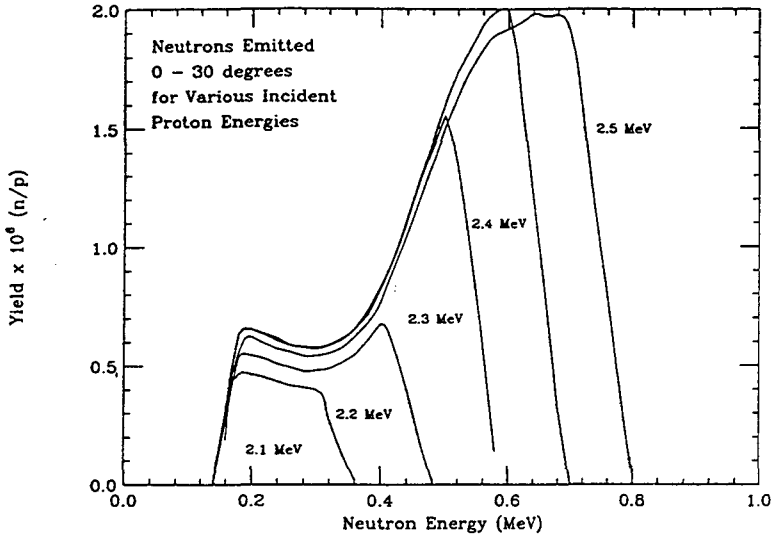

Figure 1: Neutron yields (per incident proton) for the $^{7}Li(p,n)^{7}Be$ reaction as a function of neutron energy for angles between 0° and 30° and incident proton energies between 2.1 and 2.5 MeV.

III. EPITHERMAL NEUTRON BEAM MODELING

Modeling of the neutron transport from the production target, through the moderator and filter assembly and a head phantom is necessary for evaluating neutron sources for BNCT and addressing the question of optimal proton beam energy and moderator material and thickness. Such modeling has been carried out in two stages. In the first stage the neutron beam is modeled from the $^{7}Li(p,n)^{7}Be$ source through the moderator and filter assembly using the Monte Carlo program MCNP[13]. A cross section through the three dimensional geometry specified for MCNP is shown in Fig. 2. This geometry includes a circular neutron source with a 5 cm radius and energy and angular dependencies as described in the previous section. The source is distributed uniformly across the surface of the disk corresponding to a uniform proton beam. A 1 cm thick aluminum target backing is included in the modeling, which is followed by the cylindrical moderator of variable thickness and material. Surrounding the entire moderator and proton beam port is an Al_2O_3 reflector. In preliminary studies, lead and carbon were found to be suitable but not superior as reflector materials and Al_2O_3 was used for all simulations presented in this report. Finally, all interface surfaces are lined with 0.05 g/cm^2 of ^{6}Li, in the form of either ^{6}LiF or pure ^{6}Li, for the filtering of thermal neutrons, with the exception of the exit window of the moderator, which is lined with 0.01 g/cm^2 of ^{6}Li.

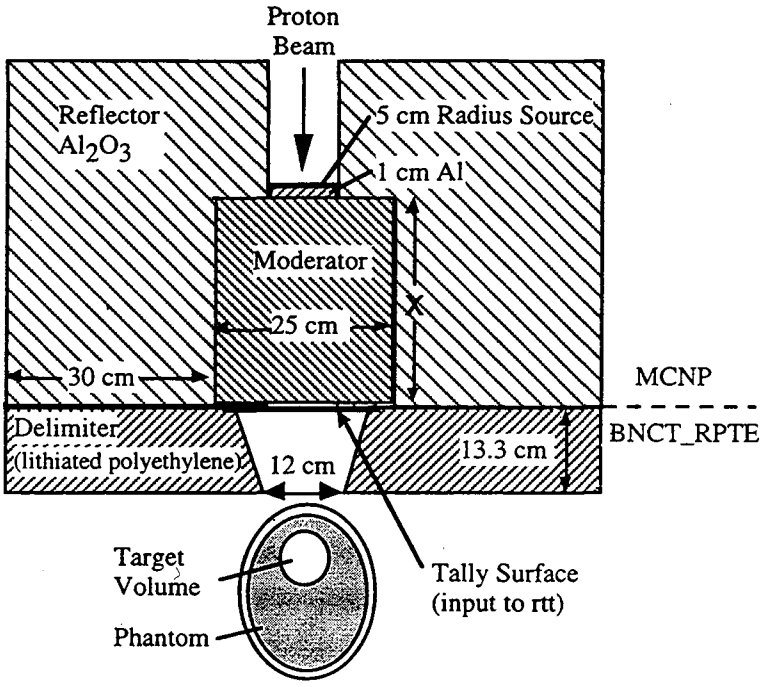

Figure 2: Cross section of moderator and filter assembly with head phantom as used for MCNP and BNCT_RTPE simulations.

Three moderator materials were analyzed. The first material, heavy water (D_2O), was chosen as it has been used in previously published studies of accelerator-based BNCT facilities[14-16]. Its advantage lies in its strong moderating capability leading to thin moderators and high dose rates. A second material, a mixture of aluminum and aluminum fluoride, has given excellent results for a BNCT beam from a TRIGA reactor[17] but, to the best of our knowledge, had not previously been applied to an accelerator-based neutron source. Its ability to filter neutrons with energies above 20 keV makes it a promising choice for BNCT applications. A mixture of 60% AlF_3 and 40% Al was assumed for all simulations. The third material, enriched ^7LiF, has been shown in a previous study[18] to have excellent moderating and filtering properties.

The energy and angular dependent neutron and photon distributions are determined by MCNP across a 20 cm surface at the exit of the moderator. These distributions are used as the source for a second Monte Carlo model, simulating the radiation transport through a delimiter and head phantom, as discussed below. The complete history of particles crossing the moderator exit is stored in the form of an MCNP binary runtape file. Using an ancillary routine supplied by INEEL personnel the file is converted into a

format featuring ten equal-intensity angle bins and 5 energy bins per decade, that can be used as input to the treatment planning software BNCT_RTPE[19].

Each moderator produces a neutron spectrum of characteristic shape, examples of which are shown in Fig. 3 along with a typical spectrum produced by the Brookhaven Medical Research Reactor (BMRR). The distributions for the Al/AlF_3 and the ^{7}LiF moderators are relatively narrow exhibiting a maximum between 10 keV and 20 keV and sharp falloffs towards higher and lower energies. In contrast, the D_2O moderated beam shows a much broader distribution with its maximum at about 1 keV. The BMRR spectrum is also broad with a maximum around 100 eV. These spectral variations suggest differences in the clinical properties of the beams.

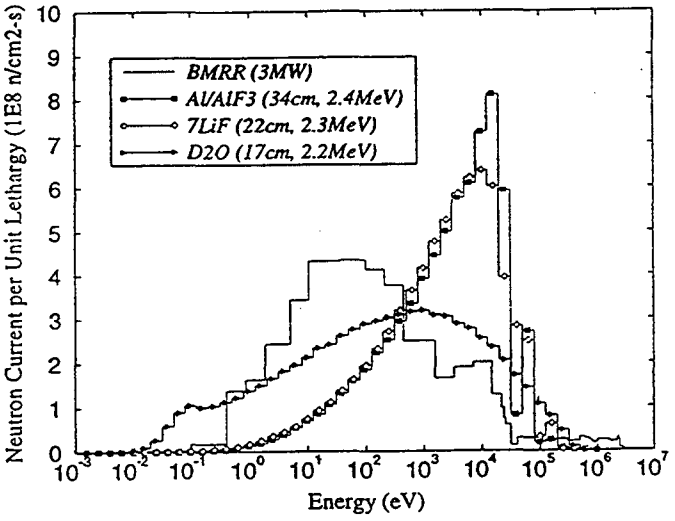

Figure 3: In-air neutron spectra for Al/AlF_3, ^{7}LiF, D_2O moderated beams and the BMRR beam. The spectra were normalized to equal total neutron fluence at the exit surface of the moderator.

The transport of neutrons and photons through a head phantom has been analyzed in the second modeling stage using the special-purpose BNCT Radiation Treatment Planning Environment (BNCT_RTPE) software system[19,20] developed by the Idaho National Engineering and Environmental Laboratory (INEEL) and utilized in the clinical trial at the BMRR. The geometry and setup is depicted in Fig. 2. It includes a lithiated polyethylene beam delimiter like the one developed for the BMRR beam[21] and a head phantom at a distance typical for clinical setups. In this study the CT-based description of an actual head was used as a phantom for all simulations.

The modeling was broken up into two stages for the following reasons: a) a full Monte Carlo simulation including target, moderator and filter assembly and the head phantom, would have required too much computer time, b) using BNCT_RTPE to simulate the in-phantom radiation transport allowed us to calculate all quantities of interest such as thermal neutron fluences and dose distributions, c) in BNCT_ RTPE Relative Biological Effectiveness (RBE) factors can be applied and total equivalent dose distributions calculated and compared, d) using a description of the BMRR epithermal beam[22] as input for BNCT_RTPE facilitated a straightforward comparison with the reactor beam. For the neutron transport simulations in BNCT_ RTPE a 10 ppm ^{10}B concentration was assumed. The normal tissue and tumor ^{10}B doses were determined by scaling to their respective concentrations.

IV. CLINICAL REQUIREMENTS AND FIGURES -OF-MERIT

In BNCT the tumor dose is boosted by a high ^{10}B concentration in the tumor cells. However, several background reactions contribute equally to the dose to normal tissue and tumor. Thermal neutrons produce the so-called nitrogen dose (D_N) through the $^{14}N(n,p)^{14}C$ neutron capture reaction. They are also the main contributor to the γ dose ($D\gamma$) via the $^{1}H(n,\gamma)^{2}H$ capture reaction. For neutron energies above about 1 keV the energy transfer to the tissue is dominated by the generation of recoil protons. The proton-recoil dose D_r is strongly dependent on the energy spectrum of the neutron beam. The goal of the moderator and filter design is to limit this contribution while maximizing the penetration of the beam and the total dose rate.

A. Equivalent-dose computation

The evaluation of the clinical efficacy of epithermal neutron beams for BNCT requires the calculation of the dose distributions in tumor and normal tissues. This task is complicated by the fact that the various kinds of radiation contributing to the total dose have different biological effectiveness. Furthermore, the biological effectiveness of the physical dose due to neutron capture by the ^{10}B nuclei (D_B) depends on compound specific properties, such as the microscopic distribution of ^{10}B, and, therefore, so called compound factors (CF) have been introduced. Using CF and RBE one can add the different dose components and express the total photon equivalent dose (D_{tot}) in gray-equivalent (Gy-Eq) units:

$$D_{tot} = CF \cdot D_B + RBE_N \cdot D_N + RBE_r \cdot D_r + RBE_\gamma \cdot D_\gamma \quad (4)$$

In general, RBE and CF are dependent on the biodistribution characteristics of the boron-carrying pharmaceutical, the neutron energy spectrum, and the biological endpoint under consideration. For this study the dose calculation protocol[23] developed for the BNCT clinical trial at the BMRR was adopted and boron concentrations and compound factors as established for the boron compound boronphenylalanine (BPA) were used. The values listed below were used for all dose calculations: normal tissue ^{10}B concentration: 13 ppm; normal tissue compound factor: 1.3; tumor ^{10}B concentration: 45.5 ppm; tumor compound factor: 3.8; proton-recoil RBE (RBE_r): 3.2; nitrogen capture RBE (RBE_N): 3.2; and γRBE (RBE_γ): 1.0. With this approach an established clinical protocol was followed and direct comparisons with treatments under the BMRR protocol were made possible. It should be noted that the neutron RBE values (RBE_r, RBE_N) were experimentally determined for the BMRR beam and that, in general, the values are expected to differ for a beam with a different neutron spectrum. Blue et al.[24] have investigated the RBE of neutrons as a function of neutron energy. Using their empirical relationship (Fig. 6 in Ref. 24) the spectrum averaged neutron RBE values for the BMRR beam and the accelerator-produced beams (for the neutron spectra shown in Fig. 3) were estimated. The averaged neutron RBE values for the Al/AlF_3 and ^7LiF moderated beams were 10% - 15% lower than for the BMRR beam indicating that the equivalent neutron dose and, therefore, the normal tissue dose may be overestimated for the accelerator-produced beams. However, differences of this magnitude do not significantly influence the results of this paper and possible differences in neutron RBE values were neglected.

B. Clinical requirements

The discussion in this paper is restricted to single beam treatments of brain tumors although in practice two or more fields, e.g., parallel opposed ports, are more likely to be used. As the most important clinical requirement the dose to the healthy brain tissue must be kept below its tolerance limit. Following the BMRR protocol the maximum equivalent dose to the normal brain was set to 12.5 Gy-Eq. As a second clinical requirement an upper limit was imposed on the entrance surface dose. This was necessary since the proton-recoil dose is highest at the skin but diminishes rapidly with increasing depth. For the purpose of the study we adopted a very simple procedure by setting the entrance dose limit to 10 Gy-Eq as calculated for normal brain tissue at a

depth of 0 cm. This accomplished two goals: first, this value ensures that when considering differences in ^{10}B concentration (skin/blood ratio for BPA of 1.3 - 1.5) and relative biological effectiveness and compound factors (BPA: ~2.5 for moist desquamation and ~1.0 for dermal necrosis[23]), the radiation tolerance for the scalp will not be exceeded. Secondly, this value implicitly limits the volume of the normal brain which receives a dose close to the maximum value of 12.5 Gy-Eq. Incidentally, as shown below (Sec. V.B) the chosen entrance dose limit corresponds to a moderator thickness which tends to give the highest tumor dose at depth. Doses to other organs and the whole body must be accounted for in the actual treatment planning process since they may impose limitations and may require special beam collimation and patient shielding. Preliminary results of such studies can be found in Costes et al. [25].

C. Figures-of-merit

A variety of figures-of-merit have been proposed and used in BNCT neutronics analyses. However, in-air measures of beam quality such as the "useful fluence", i.e., the integrated neutron fluence between a lower and an upper energy boundary, can be misleading. In this measure all neutrons with energies inside the boundaries are given equal weighting while neutrons outside the interval are discarded. The integrated useful fluences (1 eV $\leq E_n \leq$ 10 keV) for the spectra in Fig. 3 are within about 20% of each other. Yet one would expect a difference in clinical merit based upon the variation in the spectral shapes. It should be noted that the ratio of the useful fluence to the entrance dose equivalent (RUFTED)[14] does not reflect the relative quality of the beams in Table I either.

The beam quality can be better expressed in terms of in-phantom quantities. Often used is the advantage depth (AD) which is defined as the depth where the tumor dose is equal to the maximum normal tissue dose[26]. Although the advantage depth is a measure for the penetration of the beam, it does not directly indicate how well deeper seated tumors can be treated. As can be seen for the examples listed in Table I, a 13% increase in AD can reflect a 50% increase in the equivalent dose near the midline of the brain.

For these reasons we have focused on the equivalent dose at a depth of 8 cm (near the midline of the brain) for a given maximum equivalent dose to the normal tissue as the best indicator of beam quality. We also give equivalent dose and thermal neutron fluence at the depth of maximum tumor dose and at 5 cm depth, as well as associated treatment times.

V. ANALYSIS AND RESULTS

A. Uncertainties introduced by simplifying modeling assumptions

A number of simplifications were made in the epithermal neutron beam modeling, some of them due to the division of the simulation into two stages. The introduced uncertainties were estimated by comparing the modeling results for a reference case, 2.5 MeV protons and a 35 cm thick Al/AlF_3 moderator, to the output of a more accurate calculation performed for that case. The following is a summary of the analysis of the uncertainties introduced by simplifications and assumptions in our study:

a) Statistical uncertainty of Monte Carlo simulations

Determining the statistical uncertainty in the final results is difficult. While it is simple to determine the uncertainty of each energy bin of the MCNP output, it is very difficult to determine their effect on the uncertainty in the doses at particular depths in the phantom. Therefore, as a test, the number of particles simulated was increased by a factor of ten, both in MCNP and in BNCT_RTPE, thus reducing the statistical uncertainty by a factor of about three. The dose at a depth of 8 cm varied by less than 2% and the treatment time varied by only 0.2%.

b) Significance of γ production in aluminum

A large source of a beam's γ contamination is the $^{27}Al(n,\gamma)^{28}Al$ reaction. Aluminum is present in the reflector for all models, and makes up the bulk of the material for one moderator type. MCNP does not take into account the additional γ component due to the beta decay of the ^{28}Al (2.45 minute half life) and prompt emission of a 1.77 MeV γ ray. However, the majority of the γ dose is produced in the phantom mainly by neutron capture in hydrogen. In order to find an upper limit for the effect of the external γ contribution, the γ source intensity incident on the phantom (while maintaining the same neutron intensity) was doubled. This is a very conservative estimate, as, in particular for the moderator materials not containing aluminum, the actual increase in γ contamination by the decay of activated aluminum would be much smaller. A small change in the tissue depth dose characteristics was found, which reduced the treatment time by 3% and lowered the equivalent dose at 8 cm depth by 1.9%.

The $^{27}Al(p,\gamma)^{28}Si$ reaction is an additional source of γ rays if the proton beam penetrates the lithium layer and stops in the aluminum backing. This reaction has many resonances at low proton energies and produces γ rays in the energy range from a few keV to ~ 10 MeV[27]. In particular, there is a resonance at E_p = 992 keV which produces

~ 10^{-9} γ rays per incident proton[28]. However, the total contribution of this reaction was estimated to be less than a few percent of the average brain dose. If this external source of γ rays proves to be problematic, it can be eliminated by preventing the proton beam from stopping in aluminum.

c) Use of a particular head CT-scan as a phantom model

The neutron flux and dose distributions obtained in this analysis apply only to the particular phantom used. However, it is assumed that they are typical for a human head in the absence of extreme variations in size and shape. Furthermore, the same phantom was used in all simulations.

d) Significance of backscattered neutrons from delimiter and head phantom in the source description for BNCT_RTPE

Neutrons that backscatter off the delimiter, back into the moderator/reflector assembly, and back across the tally surface are not counted due to the breakup of the simulation into two stages. It was important to determine the effect of these neglected backscattered neutrons by running the test case in which the lithiated polyethylene delimiter was included in both MCNP and in BNCT_RTPE. The result was an increase in total neutron flux, and a corresponding 4.5% decrease in treatment time. Also, a slight softening of the neutron spectrum was observed but no observable change in the tumor dose at 8 cm depth.

e) Significance of the source simplification for BNCT_RTPE

The source input to the BNCT_RTPE program has been greatly simplified as evenly distributed over a disk with a diameter of 20 cm. All neutrons and photons outside the disk are neglected and all neutrons and photons within a 10 cm radius are assumed to be uniformly distributed. In order to test for the possible effect of this simplification, the neutron flux across the patient side of the delimiter of the simplified case was compared to the neutron flux for the actual source distribution using MCNP for the calculations. The distributions were indistinguishable.

Finally, to determine the effect of simplifications discussed in d) and e) on thermal neutron fluxes and doses at depth, two cases were examined. The first modeled the source with MCNP, starting from the original neutron source, through the filter assembly and into a 17-cm diameter sphere of water representing a head phantom, where the neutron spectrum in the center of the sphere was tallied. In the second case the simplified source normally serving as input into BNCT_RTPE, was used. The thermal flux at the

center of this sphere (8.5 cm depth) was $4.13 \cdot 10^8 \pm 8.8\%$ n/(cm^2 s) for the "true" source and $4.77 \cdot 10^8 \pm 3.0\%$ n/(cm^2 s) for the "simplified" source, corresponding to a difference of about 15%. This indicated that the two-step (MCNP to BNCT_RTPE) method did not introduce large uncertainties and, in particular, relative results can be expected to be quite accurate. It should be noted that this comparison included the effect of the simplified source, the effect from neglecting backscattered neutrons, both of which contribute to the total uncertainty of the BNCT_RTPE source, and possible differences in the neutron transport calculations between MCNP and BNCT_RTPE.

B. Results

Depth dose distributions along the central beam axis for the healthy brain tissue are shown in Fig. 4 for a 2.4 MeV proton beam and a 34 cm thick Al/AlF_3 moderator. The proton-recoil dose differs from the other contributions in that it is highest at the entrance and rapidly decreases with depth contributing less than 10% of the total at the point of maximum total equivalent dose. In general, the proton-recoil contribution, and therefore the entrance dose, is strongly dependent on the moderator thickness as is the treatment time.

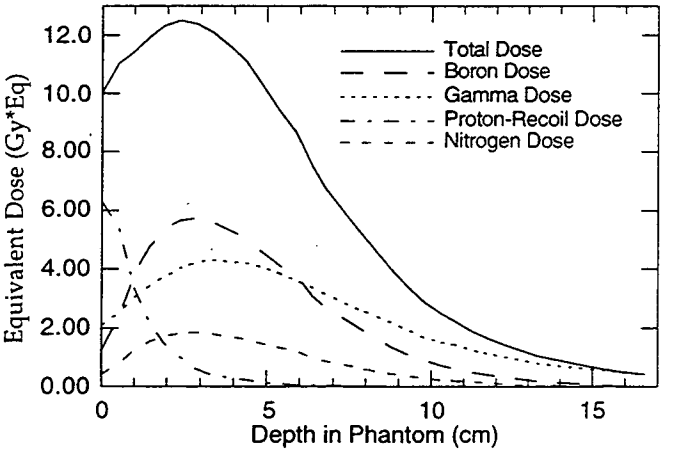

Figure 4: Normal tissue depth dose distributions in a phantom for a 2.4 MeV proton beam on a ^{7}Li target and a Al/AlF_3 moderator.

In order to find the optimal compromise for the moderator thickness for a given material and proton beam energy, in-phantom dose distributions were calculated for a set of moderator thicknesses and evaluated in terms of entrance dose, tumor doses or,

alternatively thermal fluences, at 8 cm depth, and treatment time. The treatment time is given as the time to reach the normal tissue dose limit of 12.5 Gy- Eq at a given proton beam current (20 mA). Shown in Fig. 5 are the entrance dose, tumor dose at 8 cm depth,

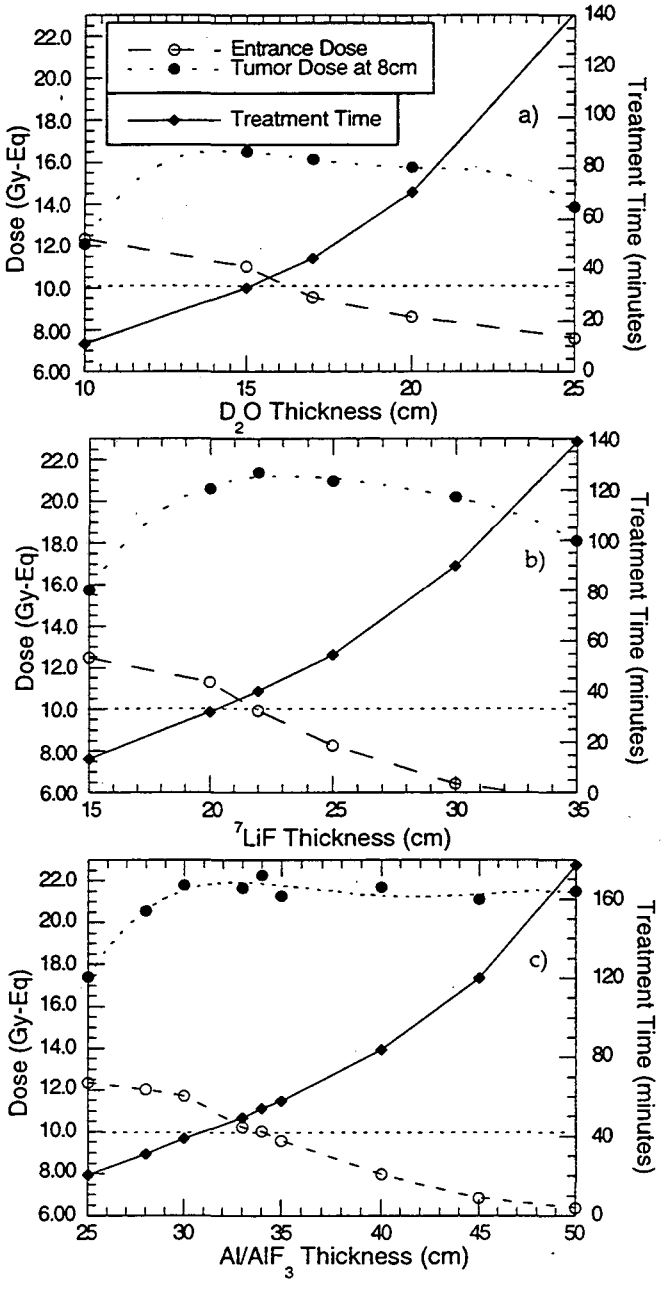

Figure 5: Entrance dose, tumor dose at 8 cm depth, and treatment time as a function of depth for a) D_2O, b) ^7LiF, c) Al/AlF_3 moderated beams.

and treatment time as function of the moderator thickness for the three moderator materials studied. The entrance dose decreases with increasing moderator thickness and drops below 10 Gy-Eq at 34 cm for Al/AlF_3, at 22 cm for ^7LiF, and at 17 cm for D_2O at the selected proton beam energies of 2.4 MeV, 2.3 MeV, and 2.2 MeV, respectively. For all three moderators the tumor dose at 8 cm depth tends to reach its maximum at roughly the same thickness at which the entrance dose reaches 10 Gy-Eq. Because the treatment time increases monotonically with moderator thickness, the minimum thickness which fulfills the requirement of an entrance dose below 10 Gy-Eq was considered optimal.

The energy of the proton beam is another variable that needs to be optimized. Based on neutron yield considerations 2.5 MeV has generally been assumed in the literature as the optimal proton beam energy. However, at a lower proton beam energy the reduction in primary neutron yield may be compensated by a reduction in moderator thickness and associated losses. Simulation studies were performed for all three moderator materials and proton energies between 2.1 and 2.6 MeV. Fig. 6 shows the tumor dose at 8 cm depth and the treatment time as function of proton beam energy. For each energy the optimal moderator thickness was chosen as described in the preceding paragraph. The tumor dose at a depth of 8 cm increases slightly with decreasing proton beam energy for the Al/AlF_3 and the ^7LiF moderators. For the D_2O moderator this parameter increases roughly linearly by 20% when the proton energy is decreased from 2.6 MeV to 2.1 MeV. For all three moderator materials the treatment time decreases with increasing proton energy. The epithermal neutron beams for the three moderators at representative proton beam energies and the BMRR beam, in its configuration at the initiation of human studies in September, 1994, are compared in Table I and Fig. 7.

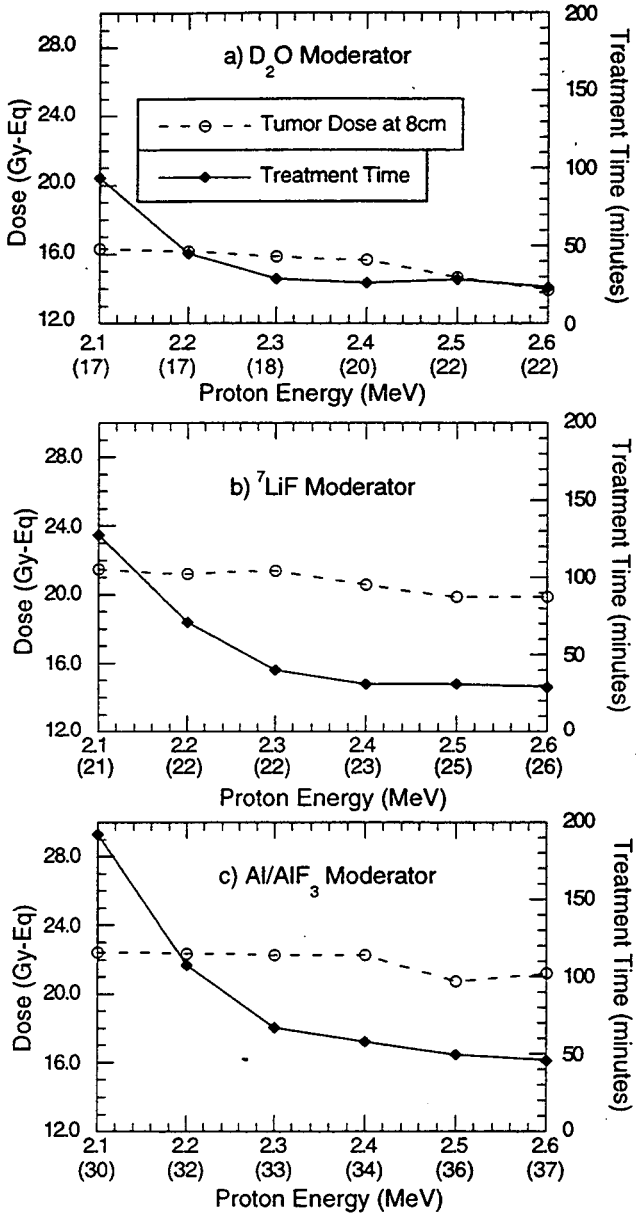

Figure 6: Tumor dose and treatment time as a function of proton beam energy for optimized a) D_2O, b) ^7LiF, c) Al/AlF_3 moderator thickness.

Table I. Comparison of accelerator-produced epithermal neutron beams and a reactor (BMRR) beam. Equivalent tumor doses and thermal fluences are given at the depth of maximum thermal fluence, 5 cm, and 8 cm.

Neutron source	$^{7}Li(p,n)^{7}Be$	$^{7}Li(p,n)^{7}Be$	$^{7}Li(p,n)^{7}Be$	BMRR
Moderator, thickness (cm)	D_2O, 17	^{7}LiF, 22	Al/AlF_3, 34	(Al_2O_3)
Proton energy (MeV)	2.2	2.3	2.4	-
Proton current (mA)	20	20	20	(3 MW)
Treatment time (min)	44	40	54	39
Equiv. tumor dose (max) (Gy-Eq.)	62.3	64.3	65.1	61.6
Equiv. tumor dose (5 cm) (Gy-Eq.)	39.1	50.5	51.4	38.6
Equiv. tumor dose (8 cm) (Gy-Eq.)	16.1	21.4	22.3	14.5
Thermal fluence (max) (n/cm^2)	$4.3 \cdot 10^{12}$	$4.5 \cdot 10^{12}$	$4.6 \cdot 10^{12}$	$4.3 \cdot 10^{12}$
Thermal fluence (5 cm) (n/cm^2)	$2.7 \cdot 10^{12}$	$3.5 \cdot 10^{12}$	$3.6 \cdot 10^{12}$	$2.6 \cdot 10^{12}$
Thermal fluence (8 cm) (n/cm^2)	$1.1 \cdot 10^{12}$	$1.4 \cdot 10^{12}$	$1.5 \cdot 10^{12}$	$9.3 \cdot 10^{12}$
Advantage depth (cm)	8.7	9.5	9.5	8.4

For the accelerator beams the treatment times for the proton energies and currents, listed in Table I and displayed in Fig. 7, range from 40 min to 54 min compared to a treatment time at the BMRR of 39 min. However, it should be noted that, as can be seen in Fig. 6, a slight increase in the proton energy can significantly shorten the treatment time while the dose near the mid-line of the brain is only slightly reduced. There are significant differences between the beams shown in Table I and Fig. 7 in their depth distributions of the thermal fluences and the tumor doses. At depths greater than 3 cm the ^{7}LiF and the Al/AlF_3 beams deposit a higher tumor dose than the BMRR beam, up to 50% more near the mid-line of the brain (8 cm depth). This is potentially a significant advantage for the treatment of deeper seated tumors given the fact that at ^{10}B concentrations currently achievable it is difficult to deliver a tumoricidal dose to these regions. The D_2O moderated beam, however, does not show this advantage. Its simulated depth dose distribution exhibits only a slight improvement over the BMRR beam. The different penetration of the beams is also indicated by the differences in the advantage depth (Table I), defined as the depth where the tumor dose is equal to the maximum normal tissue dose. The advantage depth of the ^{7}LiF and Al/AlF_3 moderated

beams of 9.5 cm is about 1 cm more than that of the BMRR beam and is close to the advantage depth found for a 12 cm diameter beam of monoenergetic (10 keV) neutrons[29].

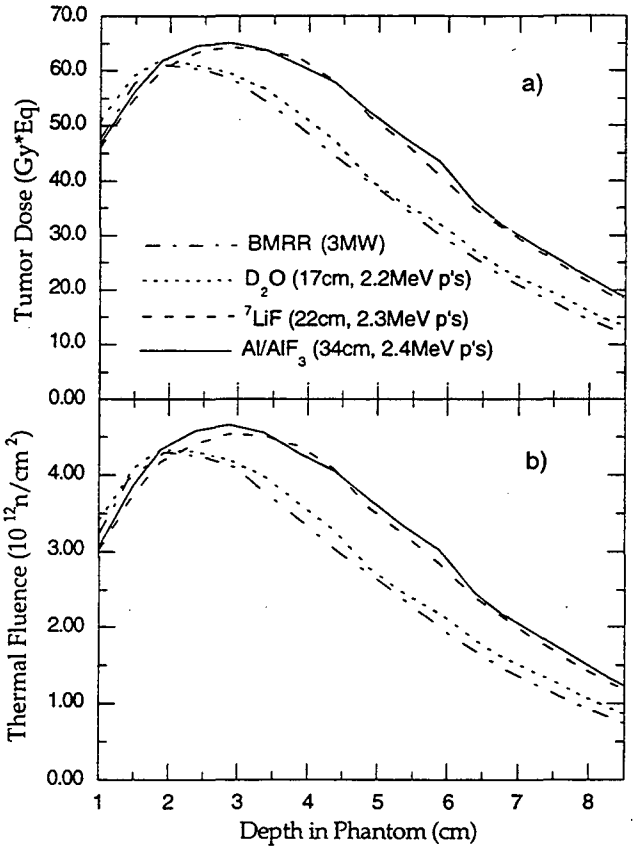

Figure 7: Depth distributions of a) total equivalent tumor doses and b) total thermal fluences for D_2O, ^7LiF and Al/AlF_3 moderated accelerator-based epithermal neutron beams and the BMRR beam.

VI. SUMMARY

Using MCNP for modeling the in-air epithermal neutron beam and BNCT_RTPE for simulating in-phantom neutron fluence and dose distributions has provided an excellent way of modeling neutron beams for BNCT, evaluating them in terms of clinical parameters, and comparing them to the BMRR beam. When utilizing the $^7Li(p,n)^7Be$ reaction as the neutron source, the choice of moderating material has an impact not only on the dose rate but also the neutron energy spectrum. D_2O requires the least amount of material and gives the shortest treatment times but ^7LiF and Al/AlF_3 produce superior neutron spectra which result in more penetrating depth dose distributions. Moderating

the reactor fission neutron spectrum requires a rather thick moderator leading to a broad neutron energy distribution across the epithermal region. The primary neutrons from the $^{7}Li(p,n)^{7}Be$ reaction at proton energies between 2.2 and 2.4 MeV have much lower maximum neutron energies, between 500 and 700 keV, than the reactor neutrons thus requiring significantly less moderation. With ^{7}LiF or Al/AlF_3 as moderating material this results in neutron spectra with rather narrow energy distributions which peak between 10 and 20 keV. As shown in this study these differences can be exploited to yield a significant increase in the tumor dose at depth compared to a reactor beam, about 30% at a depth of 5 cm and 50% at a depth of 8 cm, near the mid-line of the brain. This represents a clear clinical advantage since it is difficult to deliver a sufficient dose to tumor cells at these depths at presently achievable ^{10}B concentrations.

Previous design studies of BNCT facilities based on the $^{7}Li(p,n)^{7}Be$ reaction[14-16] chose D_2O moderators for maximizing the dose rate and minimizing treatment time. In contrast, this study has been based on the assumption that accelerator and target technologies are available which will provide a sufficient beam current to realize other options. Therefore, the epithermal neutron beam design was driven by clinical requirements and not by the desire to minimize the treatment time. It was attempted to model a practical moderator assembly including a 13 cm thick delimiter. This places the phantom surface at about 16 cm from the moderator exit surface which may account for some of the differences with previously published studies[14-16]. In summary, this study shows that based on the $^{7}Li(p,n)^{7}Be$ reaction and a proton beam current of 20 mA, brain tumor treatments with superior depth dose characteristics can be delivered in about the same time as currently required at the BMRR.

Acknowledgments

We would like to thank F. Wheeler and D. Wessol from the Idaho National Engineering Laboratory for making the BNCT_RTPE software available to us and for their extensive help in its installation and use. The authors are also indebted to C. Wemple (INEEL) for providing the MCNP to BNCT_RTPE conversion routine and to D. Nigg (INEEL) for numerous insightful discussions. Finally, we would like to acknowledge W. Chu (LBNL) and T. Phillips (UCSF) for their leadership of the LBNL/UCSF BNCT program, making this work possible.

References:

[1] J.A. Coderre, R. Bergland, J. Capala, M. Chadha, A.J.Chanana, E. Elowitz, D.D. Joel, H.B. Liu, D. Slatkin, "Boron Neutron Capture Therapy for Glioblastoma Multiforme using p-Boronophenylalanine and epithermal neutrons - trial design and early clinical results," Journal of Neuro-Oncology **33,** 93-104, 1997.

[2] W.T. Chu, D.L. Bleuel, R.J. Donahue, R.A. Gough, J. Kwan, K.-N. Leung, B.A. Ludewigt, C. Peters, T..L Phillips, L.L. Reginato, J.W. Staples, R.P. Wells, and S.S. Yu, "Design of a new BNCT facility based on an ESQ accelerator," to be published in the Proceedings of the Seventh International Symposium on Neutron Capture Therapy for Cancer, 4-7 September 1996, Zurich, Switzerland, in Excerpta Medica, International Congress Series 1132, Elsevier Science, April 1997; also LBNL Report 39519, UC-408, September 1996.

[3] J.W. Kwan, O.A. Anderson, L.L. Reginato, M.C. Vella, S.S. Yu, "A 2.5 MeV electrostatic quadrupole DC-accelerator for BNCT applications," Nucl. Instrum. Methods **B99**,710-712, 1995.

[4] J.W. Kwan , E. Henestra, C. Peters, L.L. Reginato, and S.S. Yu, "Design of a DC ESQ Accelerators for BNCT Application," Proceedings of the 14th Int. Conf. on the Appl. of Acc. in Res. & Ind., Denton Texas, November, 1996, AIP Press, New York, **Vol. II**, 1313-1315, 1997.

[5] L.L. Reginato, J. Ayers, R. Johnson, C. Peters, R. Stevenson, "Designing Power Supplies for 2.5 MeV, 100 mA d.c. for BNCT," Proceedings of the 14th Int. Conf. on the Appl. of Acc. in Res. & Ind., Denton Texas, November 1996, AIP Press, New York, **Vol. II**, 1305-1308, 1997.

[6] R.E. Shefer, R.E. Klinkowstein, J.C. Yanch, "An epithermal neutron source using a tandem cascade accelerator," in: *Progress in Neutron Capture Therapy*, Fourth International Symposium on NCT for Cancer, B. Allen, D. Moore, B. Harrington (eds.), Plenum Press, New York, 1992, 119-122.

[7] R.E. Shefer, R.E. Klinkowstein, J.C. Yanch, and W.B. Howard, "Tandem Electrostatic Accelerators for BNCT," Proceedings of the First Int. Workshop on Accelerator-Based neutron Sources for Boron Neutron Capture Therapy, Jackson, Wyoming, September 1994, **Vol. I**, 89-110. See also other contributions in these proceedings.

[8] "Heat Transfer Microstructures for Integrated Circuits," February 1984, available from NTIS, 5285 Port Royal Rd., Springfield, VA 22161.

[9] H. Liskien and A. Paulsen, "Neutron Production Cross Sections and Energies for the Reactions $^{7}Li(p,n)^{7}Be$ and $^{7}Li(p,n)^{7}Be^{*}$," Atomic Data and Nuclear Data Tables, **15**, 57-84, 1975.

[10] K. H. Beckurts and K. Wirtz, *Neutron Physics*, Springer-Verlag (1964).

[11] J.F. Janni, "Proton Range-Energy Tables, 1 keV - 10 GeV", Atomic Data and Nuclear Data Tables **27**, No. 4/5, July/September (1982).

[12] D.L. Bleuel and R.J. Donahue, "Optimization of the $^{7}Li(p,n)$ Proton Beam Energy for BNCT Application," LBNL Report, LBNL-37983, Rev. 1, May 1996.

[13] "MCNP-A A General Monte Carlo N-Particle Transport Code, Version 4A," J.F. Briesmeister, Ed., LA-12625, Los Alamos Natl. Lab., 1993.

[14] C.-K. C. Wang, T.E. Blue, R. Gahbauer, "A neutronic study of an accelerator-based neutron irradiation facility for boron neutron capture therapy," Nuclear Technology **84**, 93-107, 1989.

[15] J.C. Yanch, X.L. Zhou, R.E. Shefer, R.E. Klinkowstein, "Accelerator-based epithermal neutron beam design for neutron capture therapy," Med. Phys. **19**, 709-721, 1992.

[16] D.A. Allen and T.D. Beynon," A design study for an accelerator-based epithermal neutron beam for BNCT," Phys. Med. Biol. **40**, 807-821, 1995.

[17] I. Auterinen and P. Hiismaki, "Design of an epithermal neutron beam for the TRIGA Reactor in Otaniemi," in the Proceedings of the CLINCT BNCT Workshop, Helsinki 1993, TKK-F-A718, 14-24,1994.

[18] Y. Karni, E. Greenspan, J. Vujic, and B. Ludewigt, "Optimal Beam-Shaping Assemblies for BNCT Facilities using 2.5 MeV Protons on ^{7}Li or 19 MeV Protons on Be," Trans. of the Am. Nucl. Soc., Vol. 73, p. 29, San Francisco, CA, Oct. 29 - Nov. 2, 1995.

[19] D.W. Nigg, "Methods for Radiation Dose Distribution Analysis and Treatment Planning in Boron Neutron Capture Therapy, " Int. Journal of Rad. Onc. Bio. Phys. **28**, 1121-1134, 1994.

[20] D.W. Nigg, F. J. Wheeler, D. E. Wessol, J. Capala, M. Chada, "Computational Dosimetry and Treatment Planning for Boron Neutron Capture Therapy," Journal of Neuro-Oncology **33**, 93-104, 1997.

[21] H.B. Liu, D.D. Greenberg, J. Copala, and F.J. Wheeler, "An improved neutron collimator for brain tumor irradiations in clinical boron neutron capture therapy," Med. Phys. **23**, 2051-2060, 1996.

[22] G.K. Becker, Y.D. Harker, L.G. Miller, R.A. Anderl, and F.J. Wheeler, "Neutron Spectrum Measurements in the Aluminum Oxide Filtered Beam Facility at the Brookhaven Medical Research Reactor," in *Neutron Beam Development and Performance for Neutron Capture Therapy*, eds. O. Harling, J.A. Bernard, and R.G. Zamenhof, Plenum Press, New York and London, 1990.

[23] A.D. Chanana, "Boron Neutron-Capture Therapy of Glioblastoma Multiforme at the Brookhaven medical research reactor, A Phase I/II Study, FDA IND # 43,317, Protocol #4," Med. Dep., Brookhaven Natl. Lab., Upton, NY 11973-5000, January, 1996.

[24] T.E. Blue, J.E. Woollard, and N. Gupta, "Neutron RBE as a function of energy," 8th Intl. Conf. on Rad. Shielding, April 24-28, 1994, Arlington Texas, ANS Publishers.

[25] S.V. Costes, R.J. Donahue, and J. Vujic, "Radiation Shielding and Patient Organ Dose Study for an Accelerator-Based BNCT Facility at LBNL," LBNL Report, LBNL-39450, October 1996.

[26] R.G. Zamenhof, B.W. Murray, G.L. Brownell, G.R. Wellum, and E.I. Tolpin, "Boron Neutron Capture Therapy for the Treatment of Cerebral Gliomas. 1: Theoretical evaluation of the efficacy of various neutron beams," Med. Phys. **2**, 47-60 (1975).

[27] Y.P. Antoufiev, L.M. Nadi, D.A.E. Darwish, O.E. Badawy, and P.V. Sorokin, "Decay Scheme of the Si^{28} Nucleus," Nucl. Phys. **46**, 1-24, 1963.

[28] A. Anttila, J. Keinonen, M. Hautala and I. Forsblom, "Use of the $^{27}Al(p,\gamma)^{28}Si$, E_p=992 keV Resonance as a Gamma-Ray Intensity Standard," Nucl. Instrum. and Methods **147**, 501-505, 1997.

[29] J.C. Yanch, X.-L. Zhou, and G.L. Brownell, "A Monte Carlo Investigation of the Dosimetric Properties of Monoenergetic Neutron Beams for Neutron Capture Therapy," Rad. Res. **126**, 1-20, 1991.

Ernest Orlando Lawrence Berkeley National Laboratory
One Cyclotron Road | Berkeley, California 94720

Prepared for the U.S. Department of Energy under Contract No. DE-AC03-76SF00098